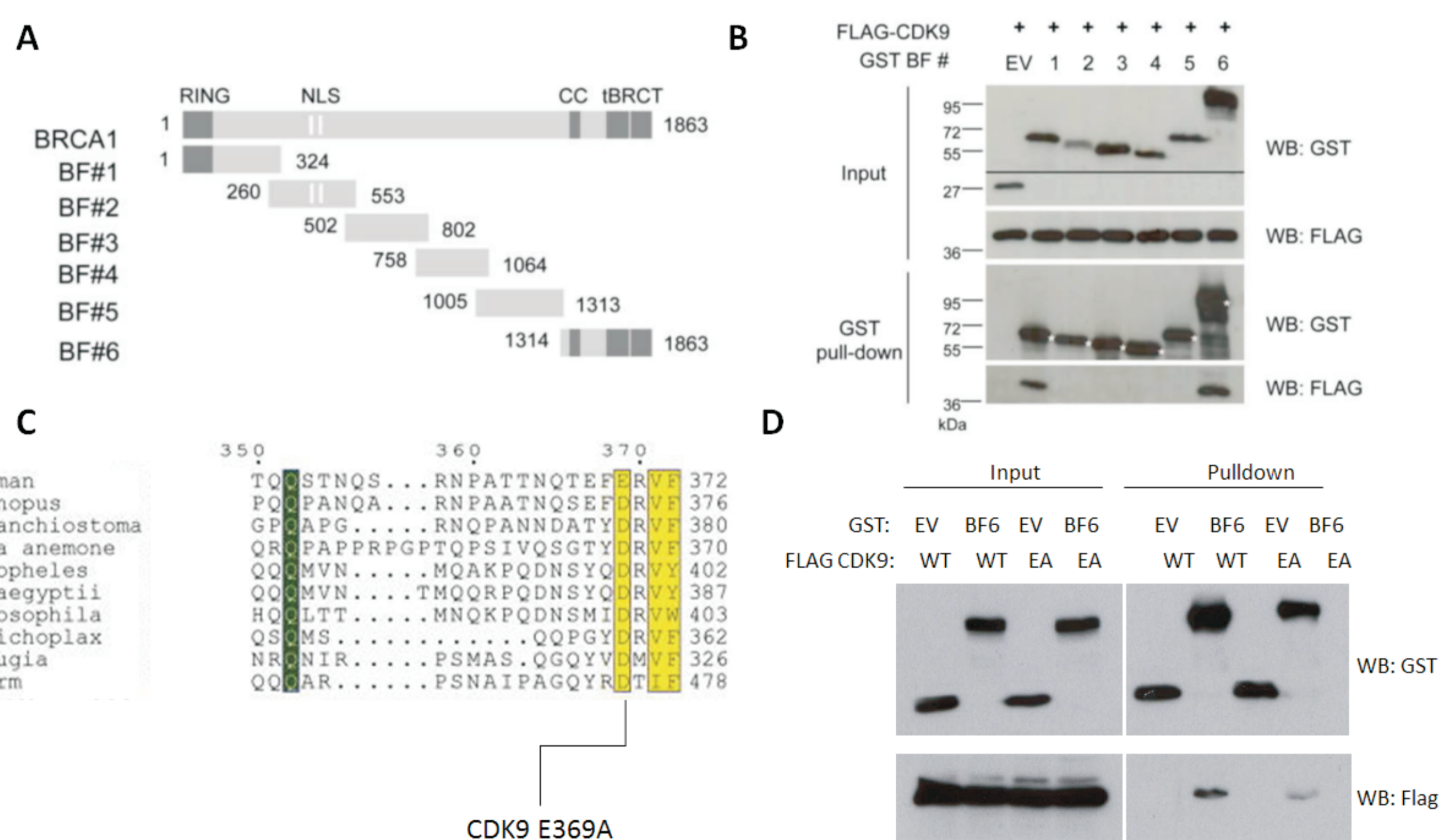


Thales C Nepomuceno<sup>1</sup>, Guilherme Suarez-Kurtz<sup>1</sup>; Alvaro N. Monteiro<sup>2</sup>, Marcelo Alex de Carvalho<sup>1,3</sup>

<sup>1</sup> Programa de Pesquisa Clínica, Instituto Nacional de Câncer, Rio de Janeiro, Brazil, <sup>2</sup> Cancer Epidemiology Program, H. Lee Moffitt Cancer Center & Research Institute, Tampa, USA, <sup>3</sup> Instituto Federal do Rio de Janeiro - IFRJ, Rio de Janeiro, Brazil

## ABSTRACT

The DNA damage response (DDR) is a well-coordinated pathway capable of sensing and repairing different types of DNA damage. Double strand break (DSB) lesions activate the ATM-CHK2 axis, which is responsible for the cell cycle arrest, prompting cells for DNA repair. DSBs are primarily repaired through two distinct pathways: homology-directed recombination (HR) and non-homologous end-joining (NHEJ). BRCA1 and 53BP1 play an important role in DDR by orchestrating the decision between HR and NHEJ, but the precise mechanisms regarding both pathways are not entirely understood. Previously, our group identified the putative interaction of the cyclin-dependent kinase (CDK9) with BRCA1 and BARD1 (BRCA1-associated RING domain 1). CDK9 is a component of the positive transcription elongation complex and has been implicated in genome integrity maintenance associated with the replication stress response. More recently, we characterized CDK9 as a DDR player by modulating BRCA1 response and consequently the HR pathway. We also demonstrated, for the first time, that CDK9 forms ionizing radiation-induced foci (IRIF) which co-localizes with BRCA1 and RPA in DNA damaged sites. Cells lacking CDK9 failure to form BRCA1 IRIF and presented a reduction in HR efficiency but not NHEJ, reflecting in increased sensitivity to IR. In the absence of CDK9, cells are deficient in RAD51 IRIF, but not 53BP1. These data corroborate the observation of reduced HR efficiency, but not NHEJ in CDK9 silenced cells. We also demonstrated that CDK9 interacts with CHK2 (apparently through the FHA domain of CHK2), another important player in the DDR pathway. Preliminary data indicate that cells lacking CHK2 are deficient in CDK9 IRIF, suggesting that CHK2 acts upstream of CDK9 in the DDR pathway. We also observed that CDK9 silenced cells are not proficient in the G2/M cell cycle arrest induced by ionizing radiation treatment. Collectively, these data place CDK9 as an important player in the DDR possibly through cell cycle checkpoint and DNA repair by HR.



**Figure 1. Structural characterization of the CDK9/BRCA1 interaction.** (A) Diagram of constructs used to map the BRCA1 interaction with CDK9. RING, RING finger domain; NLS, nuclear localization signals; CC, Coiled-coil domain; tBRCT, tandem BRCT. (B - upper panels) Co-expression of GST-fragments of BRCA1 and FLAG-CDK9 in HEK293FT cells. (B - lower panels) GST pull-down assay, Western blots (WB) were developed using indicated antibodies. (C) Orthologous alignment of CDK9 C-terminal region. Conserved position and region are highlighted in green and yellow, respectively. Adapted from Baumli *et al.*, 2012. (D - left panel) Co-expression of GST-fragment of BRCA1 (BF6) and FLAG-CDK9 wild-type (WT) or E369A (EA) mutant in HEK293FT cells. (D - right panel) GST pull-down assay, Western blots (WB) were developed using indicated antibodies.

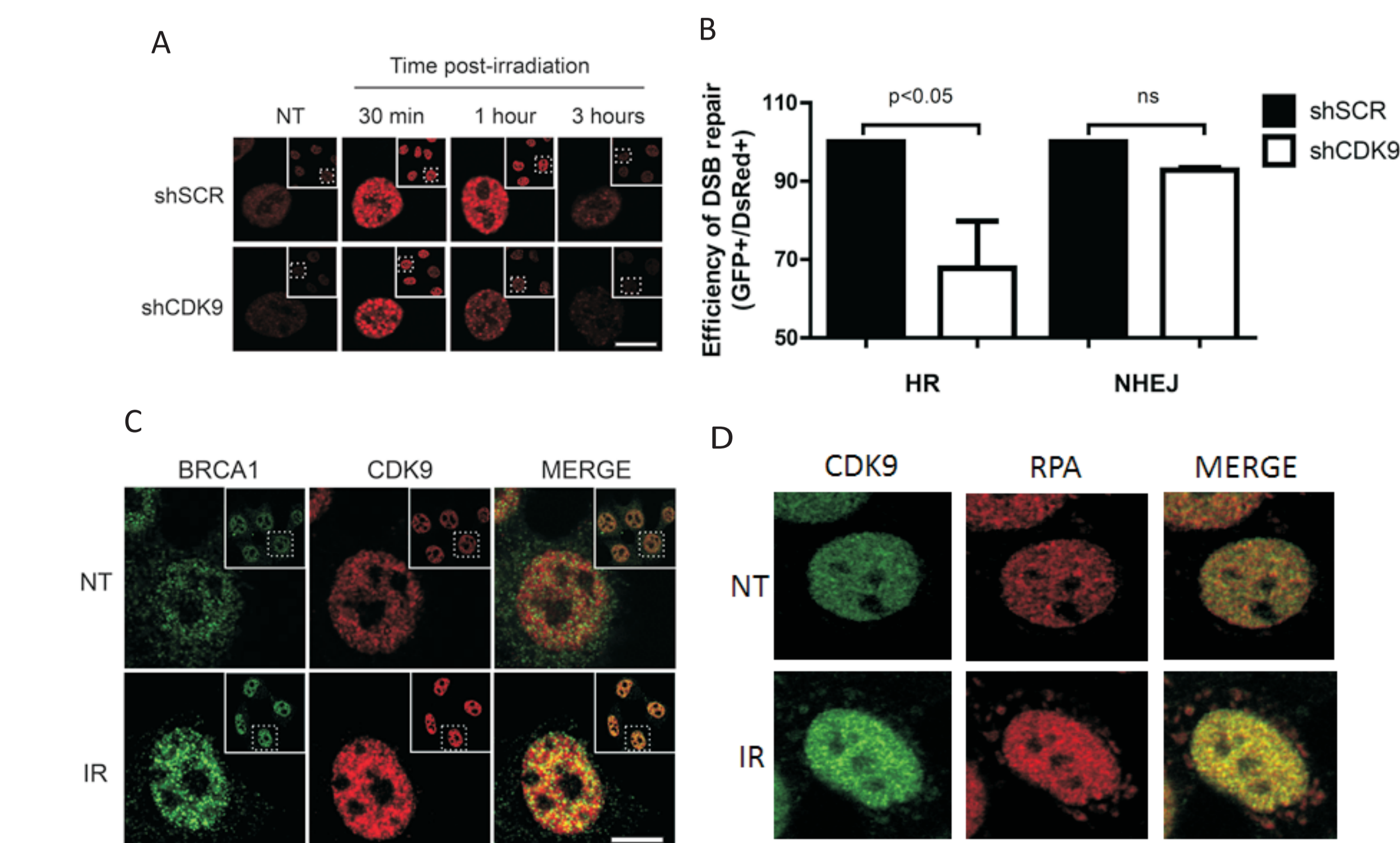


**Figure 2. CDK9 is a DDR-related protein.** (A) H2AX foci formation dynamics, CDK9-silenced cells were exposed to IR (5 Gy) and immunostained after the indicated time intervals using anti-phosphorylated H2AX (Ser139). Scale bar = 10 mm (B) HR and NHEJ repair efficiency quantification in cells lacking CDK9. Cells were analyzed 72 hours after co-transfection of linearized reporter plasmids (HR or NHEJ) and the DsRed expression vector. Data is presented as mean  $\pm$  SD of percentage of GFP positive cells relative to DsRed positive cells. CDK9 IRIF co-localization with BRCA1 (C) and RPA (D) at damaged DNA sites. MCF7 cells were exposed to IR (10 Gy) and recovered for 3 hours. Immunostaining was performed using indicated antibodies. Insets depict the nucleus in lower magnification. IR, Ionizing radiation treatment. NT, not treated. Scale bars = 10 mm.

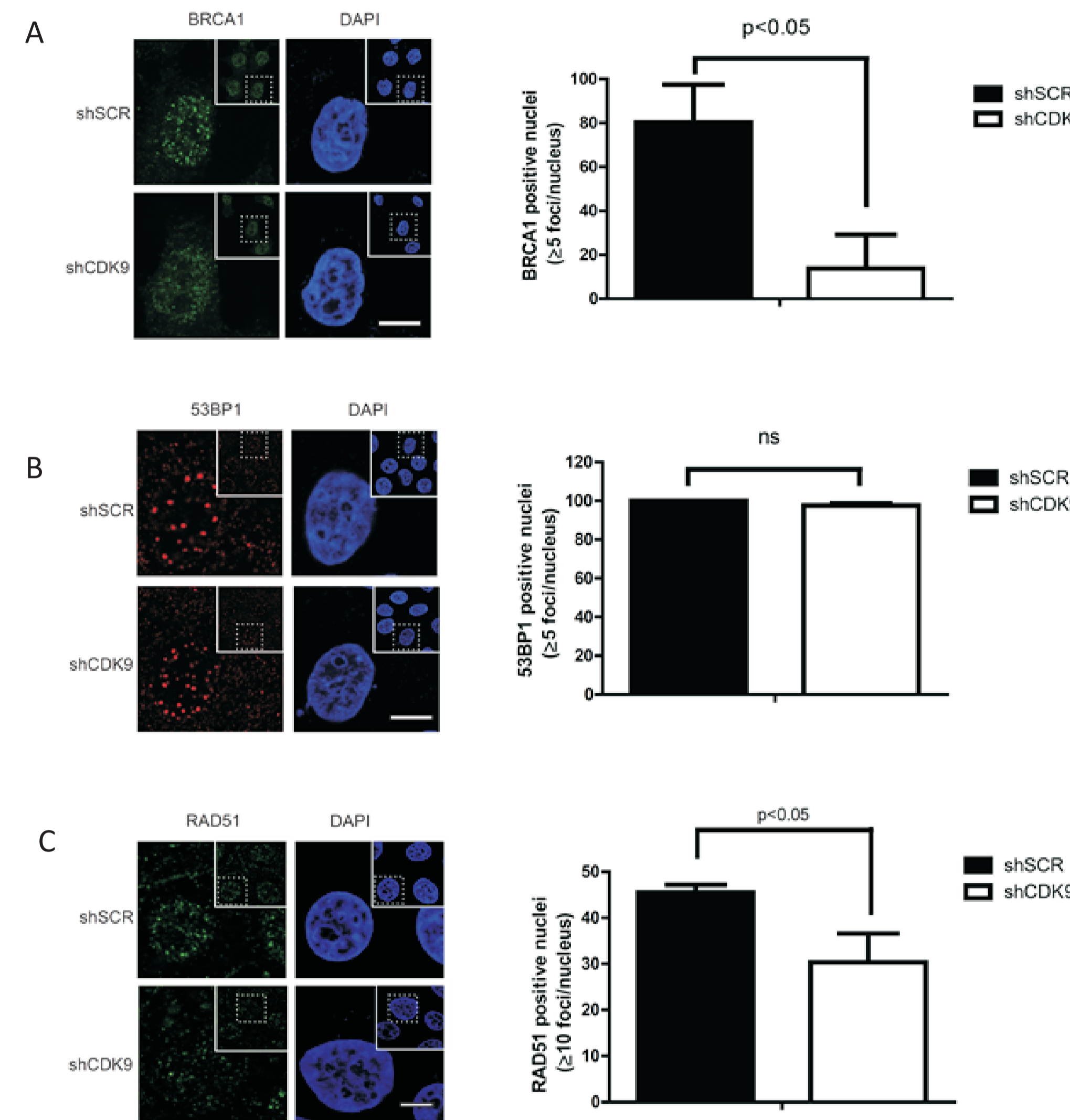


**Figure 3. BRCA1 and RAD51, but not 53BP1, recruitment to damaged DNA sites are dependent upon CDK9.** MCF7 shSCR or shCDK9 cells were exposed to IR (10 Gy) and recovered for 3 hours (A and B) or for 5 hours (C). (Left panels) Immunofluorescence staining using anti-BRCA1, anti-53BP1 or anti-RAD51. Scale bars = 10 mm. (Right panels) BRCA1, 53BP1 and RAD51 foci quantification using Image J software. Data is presented as mean  $\pm$  SD.

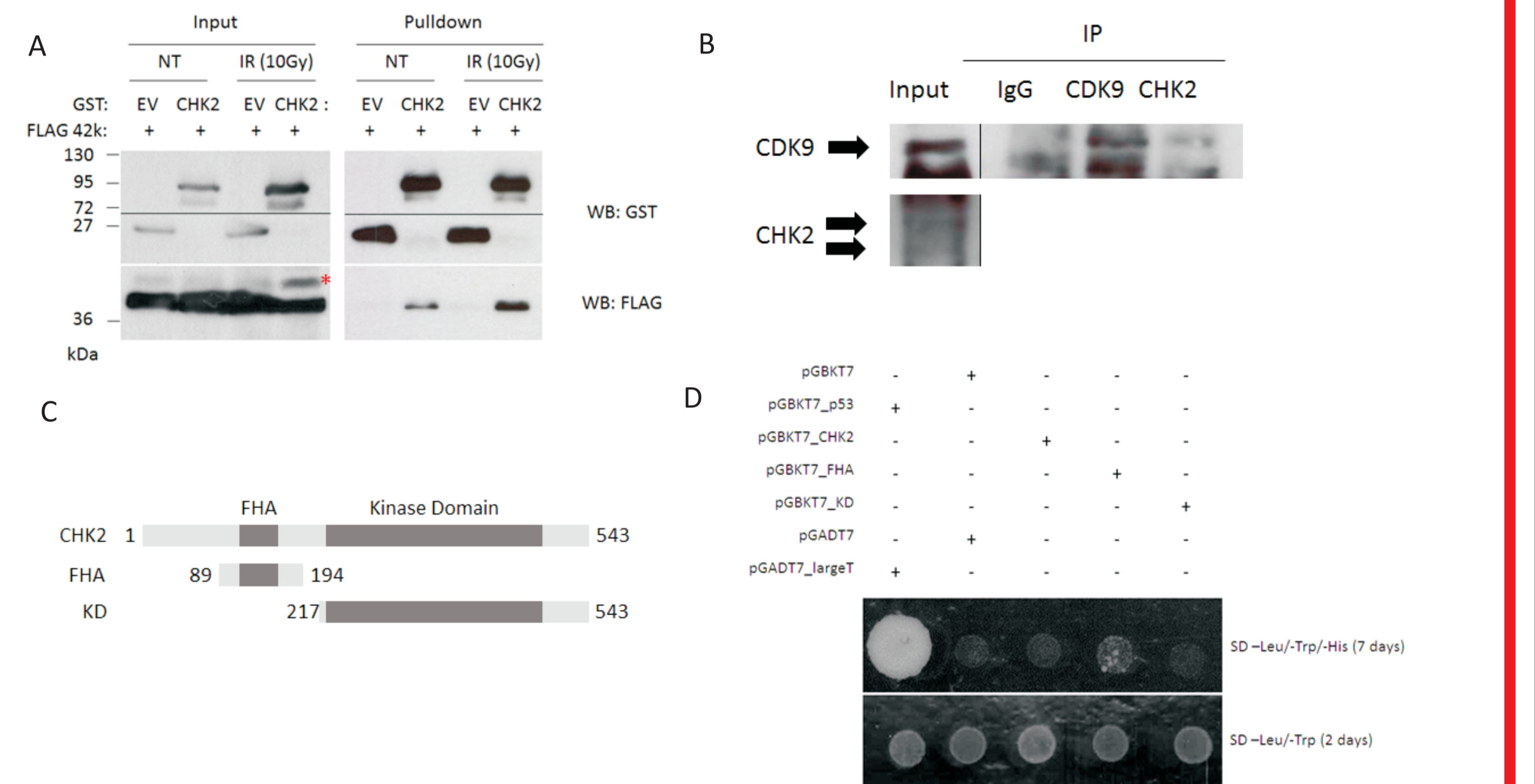


**Figure 4. Structural characterization of the CDK9/CHK2 interaction.** (A - left panel) Co-expression of GST-tagged CHK2 and Flag-tagged CDK9 in HEK293FT cells. (A - right panel) GST pull-down assay and Western blots (WB) were developed using indicated antibodies. The asterisk indicates a putative post-translational modification of Flag-tagged CDK9. (B) Co-immunoprecipitation assays were performed using HEK293FT nuclear extracts and anti-CDK9 or anti-HA (IgG) antibodies, immunoblots were developed using anti-CDK9 and anti-CHK2 antibodies, as indicated. (C) Diagram of constructs used to map the CHK2 interaction with CDK9. FHA, forkhead-associated domain; KD, kinase domain. (D) Yeast two-hybrid assay. MATa (Y2Hgold strain) and MAT<sup>-</sup> (Y187strain) cells were transformed with pGBKT7 or pGADT7 expressing vectors, respectively. After mating, diploid cells were plated in selective media (SD -Leu/-Trp or SD -Leu/-Trp/-His) for protein-protein interaction evaluation.

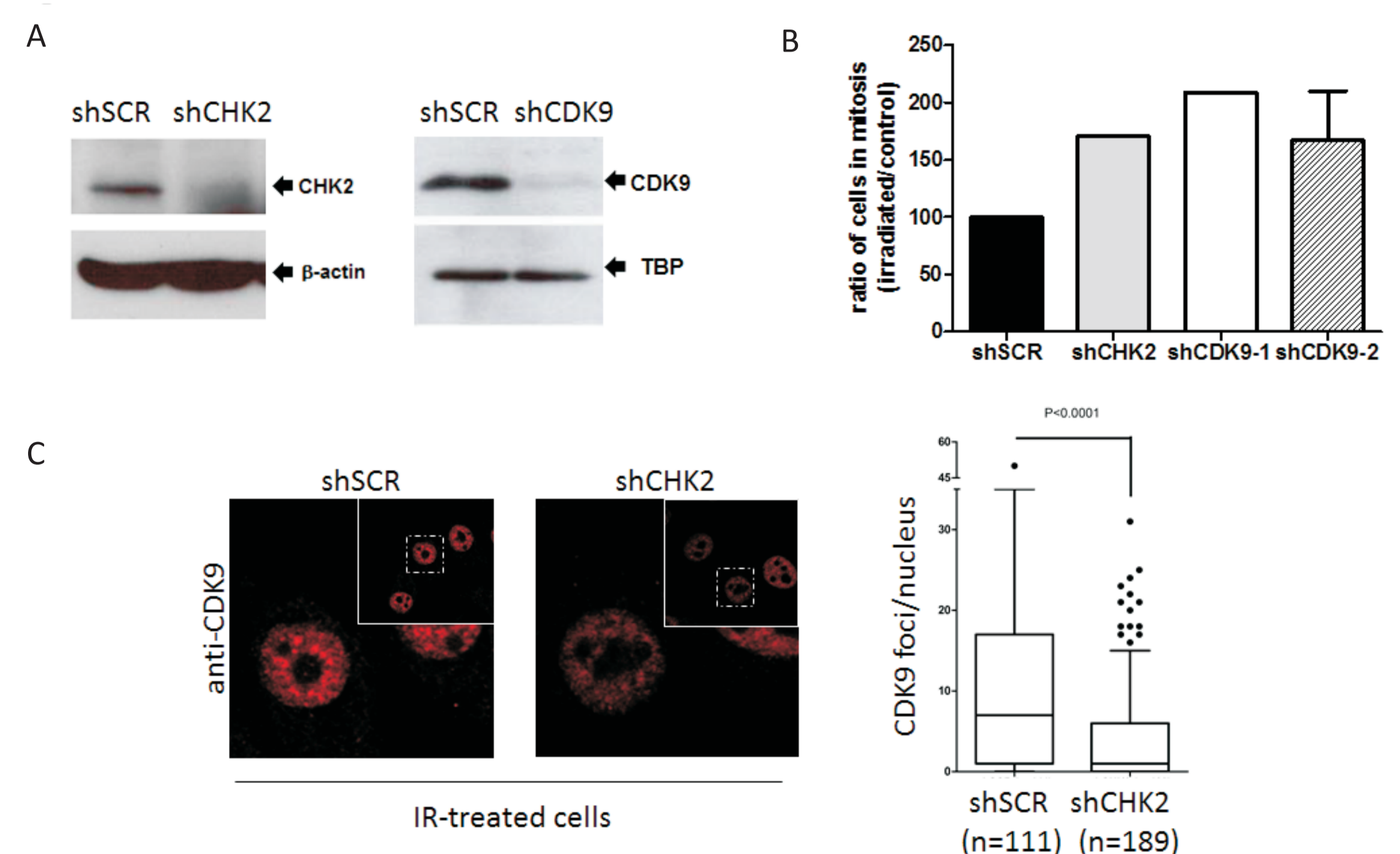


**Figure 5. Functional characterization of CDK9/CHK2 interaction** (A - left panel) CHK2 expression profile in MCF7 shSCR (negative control) and MCF7shCHK2 whole cellular extracts.  $\beta$ -actin was used as loading control. (A - right panel) CDK9 expression profile in MCF7 shSCR (negative control) and MCF7shCDK9 nuclear extracts. TBP was used as loading control. (B) Quantification of M-phase entry in IR-treated cells. MCF7 shSCR, shCDK9 and shCHK2 cells were exposed to IR (2 Gy) and recovered for 4 hours in nocodazole. Mitotic cells were analyzed using anti-phosphorylated H3 at Ser28. (C) MCF7 shSCR or shCHK2 cells were exposed to IR (10 Gy) and recovered for 3 hours. (Left panel) Immunofluorescence staining using anti-CDK9. (Right panel) CDK9 foci quantification using Image J software.